

A stochastic correlation extension of the Vasicek credit risk model

Dhruv Bansal^{*1}, Mayank Goud^{†2}, and Sourav Majumdar^{‡3}

¹Department of Aerospace Engineering, Indian Institute of Technology Kanpur, India

²Department of Economic Sciences, Indian Institute of Technology Kanpur, India

³Department of Management Sciences, Indian Institute of Technology Kanpur, India

Abstract

In the Vasicek credit portfolio model, tail risk is driven primarily by the asset-correlation parameter, yet empirically is subject to correlation risk. We propose a stochastic correlation extension of the Vasicek framework in which the correlation state evolves as a diffusion on the circle. This representation accommodates both non-mean-reverting and mean-reverting dependence regimes via circular Brownian motion and von Mises process, while retaining tractable transition densities. Conditionally on a fixed correlation state, we derive closed or semi-closed form expressions for the joint distribution of two assets, the joint first-passage (default) time distribution, and the joint survival probability. A simulation study quantifies how correlation volatility and persistence reshape joint default-at-horizon, survival, and joint barrier-crossing probabilities beyond marginal volatility effects. An empirical illustration using U.S. bank charge-off rates demonstrates economically interpretable time-variation in a dependence index and shows how inferred stochastic dependence translates into materially different joint tail-event probabilities. Overall, circular diffusion models provide a parsimonious and operationally tractable route to incorporating correlation risk into Vasicek structural credit calculations.

Keywords: Credit Risk, Stochastic Correlation, Asset Correlation, Basel IRB, Portfolio Loss distribution, Correlation Risk

*dbban3961@gmail.com

†mayankgoud344@gmail.com

‡souravm@iitk.ac.in

1 Introduction

Credit portfolio risk is at its core a dependence problem: even when marginal default probabilities are well estimated, portfolio tail risk is driven by how defaults cluster under common economic stress. There are two main modelling paradigms for default risk (Bakshi et al., 2022): structural models and reduced-form (intensity-based) models. The first structural model for credit risk is due to Merton, 1974. In a portfolio setting, Vasicek, 2002 extends the Merton framework to a large pool of obligors and derives default probabilities conditional on a single systematic factor. In the large homogeneous portfolio limit, the model yields a closed-form distribution for the portfolio default rate (the Vasicek distribution), enabling tractable calculations of portfolio VaR, regulatory capital, and tranche loss probabilities Vasicek, 2002.

The analytic tractability of the Vasicek limit has shaped both industry practice and regulation. Gordy, 2003 shows that portfolio-invariant capital charges arise naturally under an asymptotic single-factor setting, and the Basel II Internal Ratings-Based (IRB) risk-weight functions are explicitly motivated and explained using this asymptotic single risk factor (ASRF) idea (Basel Committee on Banking Supervision, 2005). A central design requirement of the IRB framework is portfolio invariance (Gordy, 2003), namely that the capital charge for a given exposure should depend only on that exposure’s risk characteristics and not on the composition of the rest of the portfolio. This property is achieved in the large, well-diversified portfolio limit under a single systematic factor structure, leading directly to the Vasicek distribution for portfolio default rates. Within this structure, the asset correlation parameter governs the degree of default clustering under stress and therefore plays a pivotal role in determining tail loss quantiles and regulatory capital.

Recent supervisory analysis further highlights the central role of correlation in regulatory capital. In particular, the EBA staff paper on calibration of the IRB supervisory formula emphasises that the level of capital generated by the IRB approach depends crucially on the asset correlation parameter: it directly enters the supervisory risk-weight function and governs the mapping from expected probability of default (PD) to stressed (worst-case) default rates (Casellina et al., 2023). Because the supervisory formula effectively produces a stressed default rate through the interaction of PD and asset correlation, even modest misspecification of dependence can materially affect capital requirements. This observation reinforces that correlation is not a secondary modelling choice but a structural driver of tail loss quantiles in the ASRF framework.

In the classical Vasicek formulation the asset correlation parameter ρ is constant. However, default dependence is empirically and economically state-dependent: correlations tend to rise in stressed conditions, and uncertainty in dependence itself is often referred to as correlation risk. Concerns about the cyclicity of Basel-style credit capital have long been recognised. For example, simulations in Goodhart and Segoviano, 2004 show that, during periods of strong growth, the IRB approach can imply lower capital adequacy requirements, whereas in recessions the required capital is markedly higher, producing substantially greater cyclical variation under IRB than under alternative approaches. They conclude that “procyclicality may well still be a serious problem with Basel II” despite attempts to smooth the risk-weight curves. A related supervisory concern is that internal ratings-based capital may move mechanically with the cycle: Corcóstegui et al., 2003 argue that this can translate into lower capital requirements in favourable conditions and higher requirements in unfavourable ones,

potentially inducing banks to tighten credit in recessions and thereby amplify downturns. Using a rating system estimated over a business cycle, they quantify how obligor grade migrations driven by macro conditions translate into changes in capital required under Basel proposals.

Supervisors have also emphasised model-risk channels within ASRF implementations. Tarashev and Zhu, 2008 note that the ASRF model underpins the IRB approach and that its portfolio-invariance property relies on the single-factor and perfect-granularity assumptions. They show that, while violations of these assumptions can be relatively minor for large portfolios, plausible calibration errors in asset-return correlations (both in their level and in their dispersion) can generate economically significant inaccuracies in portfolio credit-risk measures and capital. This motivates treating dependence itself as a source of risk and modelling correlation dynamics rather than fixing a single constant correlation input.

Empirical evidence further underscores that correlation is neither constant nor innocuous. Düllmann et al., 2007 document considerable fluctuation in asset correlation estimates across portfolios and show that averaging correlation parameters can lead to substantial underestimation of portfolio VaR. In the Basel II context, Lopez, 2002 emphasises that the ASRF framework is integral to regulatory capital determination and that the average asset correlation is a key regulatory parameter linking obligor-level PDs to portfolio tail risk. More recently, Lee et al., 2011 provide evidence that asset correlations exhibit asymmetric and procyclical behaviour: correlations rise during downturns and are negatively related to default probability while being positively related to firm size. Taken together, these findings suggest that treating correlation as a fixed input may mask systematic dependence dynamics precisely when tail clustering risk is most relevant.

Correlation risk is a concern across many problems in finance. In Gaussian factor/copula settings, this motivates models in which effective dependence varies across states, maturities, or market regimes. A large literature in credit derivatives introduces random factor loadings or stochastic and local correlation precisely to reproduce observed tranche/skew behaviour and stress-dependent clustering; see, e.g., Andersen and Sidenius, 2004; Burtschell et al., 2007; Hull et al., 2005. From a risk-measure perspective, allowing correlation to move randomly transforms the loss distribution from a single Vasicek law into a mixture over correlation states, typically thickening tails and amplifying extreme-quantile sensitivity.

Several stochastic correlation models have been considered in the literature, including bounded functionals of Brownian motions (Teng et al., 2016a; Teng et al., 2016b), Wishart processes (Asai and McAleer, 2009; Da Fonseca, Gnoatto, and Grasselli, 2015; Da Fonseca and Grasselli, 2011; Da Fonseca, Grasselli, and Ielpo, 2011; Da Fonseca, Grasselli, and Ielpo, 2014; Fonseca et al., 2007; Gnoatto and Grasselli, 2014; Grasselli and Miglietta, 2016), and Jacobi processes (Ma, 2009). These approaches capture time-variation in dependence, but may lead to specifications in which ensuring $\rho \in [-1, 1]$ and retaining tractable transition densities requires careful modelling choices.

A key regulatory design constraint is operational tractability. In ASRF framework, idiosyncratic risk is assumed to be diversified away and a single systematic source drives dependence, so that capital charges admit analytical expressions. As Gordy and Lütkebohmert, 2013 stress, simple closed-form capital rules are preferred in regulatory settings for transparency, verifiability, and ease of implementation across institutions.

At the same time, concentration risk and correlation structure are precisely where real portfolios depart from the ASRF benchmark: the Basel Committee’s Research Task Force notes that concentration risk violates one or both key ASRF assumptions: name concentration implies less than perfect granularity, while sector concentration implies that risk may be driven by more than one systematic factor Basel Committee on Banking Supervision, 2006. The same report highlights that producing stable and reliable estimates of asset correlations across exposures is a key practical issue. These considerations motivate dependence extensions that remain analytically transparent and computationally efficient.

We exploit the geometric identity that the Pearson correlation between centred vectors can be written as $\rho = \cos \theta$, where θ is the angle between them. Accordingly, we model dependence as

$$\rho_t = \cos(\theta_t), \quad \theta_t \in \mathbb{S}^1,$$

where θ_t is a diffusion on the circle. This yields a bounded ρ_t by construction and leverages tractable transition densities for circular diffusions, including circular Brownian motion and mean-reverting von Mises dynamics Majumdar and Laha, 2024. We seek to exploit this tractability to derive closed-form or semi-closed-form expressions for joint default, joint survival, and joint first-passage probabilities under stochastic correlation, and to quantify via simulation and empirical illustrations how stochastic dependence alters tail risk relative to constant-correlation Vasicek benchmarks.

Section 2 introduces the stochastic-correlation extension of the Vasicek credit risk model. We model dependence through a bounded correlation process generated by a circular diffusion and derive the main conditional building blocks needed for joint credit calculations: a semi-closed form expression (via Laplace approximation) for the joint distribution of two asset values, a joint first-passage-time (default) density for the two-name barrier model, and a representation of the joint survival probability based on a killed transition density. Section 3 provides a simulation study that isolates the effect of correlation dynamics by varying the volatility and persistence parameters of the circular diffusion and quantifies the resulting changes in joint default-at-horizon, joint survival, and joint barrier-crossing probabilities relative to marginal volatility effects. Section 4 presents an empirical illustration using U.S. bank charge-off rates: we infer a time-varying effective ASRF dependence index from the Vasicek likelihood, summarise its cross-category heterogeneity and time variation, and translate the estimated dependence dynamics into joint tail-event probability calculations. Section 5 concludes and discusses limitations and directions for future work.

2 Model

We consider the setup in Vasicek, 2002. Assume that a loan portfolio has n borrowers with maturity at time T . Let $S_{i,t}$ denote the value of the i -th ($1 \leq i \leq n$) borrower at time $0 \leq t \leq T$. The evolution of the value of the asset of the i -th individual is given by,

$$dS_{i,t} = \mu S_{i,t} dt + \sigma S_{i,t} dW_{i,t}$$

We assume that at each time t , the correlation among all borrowers in a portfolio is ρ_t . That is,

$$dW_{i,t} dW_{j,t} = \rho_t dt, 1 \leq i \leq j \leq n, i \neq j$$

This is an extension of Vasicek, 2002 wherein it was considered that $\rho_t = \rho$ for all time. We say that borrower i defaults when the value of the asset of i falls below the obligated loan amount B_i , i.e., the event $A_{i,t} < B_i$ takes place at some time t . Let L denote the proportion of defaults in a portfolio, with $L_i = 1$ if borrower i defaults and $L_i = 0$ if the borrower doesn't default.

$$L = \sum_{i=1}^n w_i L_i \quad (1)$$

where $\sum_{i=1}^n w_i = 1$ and it is further assumed that $\sum_{i=1}^n w_i^2 \rightarrow 0$. The assumption is to ensure that the portfolio contains a large number of loans and the value of a few loans don't exceed that of others by much.

Proposition 2.1. *The probability density function of x percentage of defaults conditional on ρ_t in a portfolio with large number of borrowers is,*

$$f(x) = \sqrt{\frac{1-\rho_t}{\rho_t}} \exp\left(-\frac{1}{2\rho_t} \left(\sqrt{1-\rho_t}\Phi^{-1}(x) - \Phi^{-1}(\bar{x})\right)^2 + \frac{1}{2} \left(\Phi^{-1}(x)\right)^2\right) \quad (2)$$

where $\Phi(\cdot)$ is the cumulative distribution function of the standard normal distribution and $\mathbb{E}[x] = \bar{x}$.

Proof. The result for the stochastic correlation case (ρ_t) follows from Vasicek, 2002. \square

2.1 Stochastic correlation and circular diffusion models

In the single-factor Vasicek framework, the dependence parameter ρ is the primary driver of default clustering and tail loss quantiles: for fixed marginal default probabilities, larger ρ concentrates probability mass in high-default states and therefore increases joint tail-event likelihoods. Empirically, however, the strength of dependence is not constant through time and typically rises in stressed conditions. This motivates treating ρ itself as a state variable and modelling correlation risk: even if conditional credit losses remain tractable, the unconditional loss distribution becomes mixture over dependence states, often thickening tails and amplifying sensitivity of extreme quantiles.

Formally, if $Q(\rho)$ denotes any conditional quantity of interest (e.g. joint default-at-horizon, joint survival, or joint first-passage probability) computed under a fixed correlation level ρ , then under stochastic correlation its unconditional counterpart is obtained by averaging over the correlation state:

$$Q = \mathbb{E}[Q(\rho_t)] = \int Q(\rho) p_{\rho_t}(\rho) d\rho.$$

This mixture perspective is central in our approach: we derive closed/semi-closed expressions for $Q(\rho)$, and then integrate (analytically or numerically) over the distribution induced by the correlation dynamics.

A stochastic correlation model used inside structural credit calculations faces two basic constraints. First, ρ_t must remain in the admissible range $[-1, 1]$ (or $[0, 1]$ if one restricts to nonnegative ASRF dependence). Second, for the model to be operationally

useful, the transition density of the correlation state should be tractable so that mixture integrals and likelihood-based inference are feasible. Many popular specifications enforce bounds by construction (e.g. Jacobi-type diffusions on $[0, 1]$ or Wishart-based correlation matrices), but tractability can become delicate once one requires explicit transition densities and stable inference; see, e.g., Asai and McAleer, 2009; Fonseca et al., 2007; Ma, 2009; Teng et al., 2016a; Teng et al., 2016b.

We exploit the elementary geometric identity that the Pearson correlation between centred vectors can be written as a cosine of an angle,

$$\rho = \cos \theta,$$

where θ is the angle between the two centred vectors. This suggests representing the correlation state through a process on the circle,

$$\rho_t = \cos(\theta_t), \quad \theta_t \in \mathbb{S}^1.$$

This construction guarantees $\rho_t \in [-1, 1]$ without imposing reflecting boundaries, and it is particularly convenient when θ_t is chosen to be a diffusion on \mathbb{S}^1 with a known transition density. Circular diffusions and their transition laws (including wrapped normal and von Mises-type kernels) are developed and discussed in Majumdar and Laha, 2024, which we use as the backbone of the dependence specification in this paper.

In credit applications one often focuses on nonnegative dependence. This can be enforced in the same framework either by restricting the angle to $\theta_t \in [0, \pi]$ and working with $\rho_t = \cos(\theta_t)$, or (as in parts of our simulation/empirical implementation) by using the nonnegative mapping

$$\rho_t = \cos^2(\varphi_t), \quad \varphi_t \in [0, \pi/2],$$

which preserves boundedness and yields a one-to-one correspondence between $\rho_t \in [0, 1]$ and $\varphi_t \in [0, \pi/2]$.

We consider two canonical circular diffusions for the circular process.

1. Circular Brownian motion

$$d\theta_t = \sigma_\theta dW_t \pmod{2\pi},$$

which is the circular analogue of arithmetic Brownian motion. Its transition density is the wrapped normal distribution (a periodic summation of the Gaussian kernel), available in closed form as a Fourier series; see Majumdar and Laha, 2024.

2. von Mises process

$$d\theta_t = -\lambda \sin(\theta_t - \mu) dt + \sigma_\theta dW_t \pmod{2\pi},$$

which is the circular analogue of an Ornstein-Uhlenbeck process. Here λ controls persistence (mean-reversion speed) and μ is the long-run mean direction. The von Mises process admits a tractable transition density and a von Mises-type stationary distribution with concentration increasing in $2\lambda/\sigma_\theta^2$; see Majumdar and Laha, 2024.

The circular-diffusion construction provides a bounded, interpretable, and analytically convenient dependence state. Conditional on a realised correlation level ρ , joint asset values remain multivariate lognormal under our GBM asset dynamics, and key default objects can be written in closed or semi-closed form. Stochastic correlation then enters through a single additional integration or Monte Carlo averaging over the correlation state, rather than requiring full joint simulation of all obligors and factors.

Theorem 2.1 (Joint distribution of asset values).

$$f(s_1, s_2) \approx \exp(g(\gamma^*)) \sqrt{\frac{2\pi}{-g''(\gamma^*)}} \left(\Phi \left(\sqrt{-g''(\gamma^*)}(\pi - \gamma^*) \right) - \Phi \left(-\sqrt{-g''(\gamma^*)}\gamma^* \right) \right)$$

where γ^* is the solution of,

$$d \cos^3 \gamma + b \cos^2 \gamma - (a + c + d) \cos \gamma + bd = 0$$

where $a = L_1^2 \sigma^2$, $b = L_1 L_2 \sigma^2$, $c = L_2^2 \sigma^2$, $d = \sigma^4 t$ and $L_1 = \log s_1 - \log S_{1,0} - (\mu - \frac{\sigma^2}{2})t$ and $L_2 = \log s_2 - \log S_{2,0} - (\mu - \frac{\sigma^2}{2})t$,

$$g(\gamma) = -\log(2\pi\sigma^2 t \sin \gamma s_1 s_2) + \log p_\theta(\gamma) - \frac{1}{2} \frac{a - 2b \cos \gamma + c}{d \sin^2 \gamma}$$

Also,

$$g''(\gamma) = \frac{d \sin^2 \gamma - 3b \sin^2 \gamma \cos \gamma + (\cos(2\gamma) + 2)(a - 2b \cos \gamma + c)}{d \sin^4 \gamma} + \frac{p''_\theta(\gamma)}{p_\theta(\gamma)} - \frac{(p'_\theta(\gamma))^2}{(p_\theta(\gamma))^2}$$

Proof.

$$\begin{aligned} dS_{1,t} &= \mu S_{1,t} dt + \sigma S_{1,t} dW_t^{(1)} \\ dS_{2,t} &= \mu S_{2,t} dt + \sigma S_{2,t} (\rho_t dW_t^{(1)} + \sqrt{1 - \rho_t^2} dW_t^{(2)}) \end{aligned}$$

and its solution is,

$$\begin{aligned} S_{1,t} &= S_{1,0} \exp \left(\left(\mu - \frac{\sigma^2}{2} \right) t + \sigma W_t^{(1)} \right) \\ S_{2,t} &= S_{2,0} \exp \left(\left(\mu - \frac{\sigma^2}{2} \right) t + \sigma (\rho_t W_t^{(1)} + \sqrt{1 - \rho_t^2} W_t^{(2)}) \right) \end{aligned}$$

$S^{(1)}, S^{(2)}$ conditional on ρ_t jointly follows the multivariate lognormal distribution, with,

$$\Sigma = \begin{bmatrix} \sigma^2 t & \sigma^2 \rho_t t \\ \sigma^2 \rho_t t & \sigma^2 t \end{bmatrix}$$

and,

$$\Sigma^{-1} = \frac{1}{\sigma^4 t^2 (1 - \rho_t^2)} \begin{bmatrix} \sigma^2 t & -\sigma^2 \rho_t t \\ -\sigma^2 \rho_t t & \sigma^2 t \end{bmatrix}$$

The pdf is given by,

$$\begin{aligned}
& f(s_1, s_2 | \rho_t) \\
&= \frac{1}{2\pi\sqrt{\det \Sigma}} \frac{1}{s_1 s_2} \exp\left(-\frac{1}{2}(\log \mathbf{s} - \mu)^T \Sigma^{-1}(\log \mathbf{s} - \mu)\right) \\
&= \frac{1}{2\pi\sigma^2 t \sqrt{1 - \rho_t^2}} \frac{1}{s_1 s_2} \exp\left(-\frac{1}{2} \frac{L_1^2 - 2L_1 L_2 \rho_t + L_2^2}{\sigma^2 t (1 - \rho_t^2)}\right),
\end{aligned}$$

We are interested in $\mathbb{P}(S_{1,t} \leq x_1, S_{2,t} \leq x_2)$ which is,

$$\begin{aligned}
\mathbb{P}(S_{1,t} \leq x_1, S_{2,t} \leq x_2) &= \int_{-1}^1 \left(\int_0^{x_1} \int_0^{x_2} f(s_1, s_2 | r) ds_1 ds_2 \right) p(r) dr \\
&= \int_0^{x_1} \int_0^{x_2} \left(\int_{-1}^1 f(s_1, s_2 | r) p(r) dr \right) ds_1 ds_2
\end{aligned}$$

Now note the density $f(s_1, s_2)$ is given by,

$$f(s_1, s_2) = \int_{-1}^1 f(s_1, s_2 | r) p(r) dr$$

Here $p(r) = p_\theta(\cos^{-1}(r)) \frac{1}{\sqrt{1-r^2}}$

$$\begin{aligned}
& f(s_1, s_2) \\
&= \int_{-1}^1 f(s_1, s_2 | r) p(r) dr \\
&= \int_{-1}^1 \frac{1}{2\pi\sigma^2 t \sqrt{1-r^2}} \frac{1}{s_1 s_2} \exp\left(-\frac{1}{2} \frac{L_1^2 - 2L_1 L_2 r + L_2^2}{\sigma^2 t (1-r^2)}\right) p(r) dr \\
&= \int_{-1}^1 \frac{1}{2\pi\sigma^2 t \sqrt{1-r^2}} \frac{1}{s_1 s_2} \exp\left(-\frac{1}{2} \frac{L_1^2 - 2L_1 L_2 r + L_2^2}{\sigma^2 t (1-r^2)}\right) \frac{1}{1-r^2} p_\theta(\cos^{-1}(r)) dr \\
&= \int_0^\pi \frac{1}{2\pi\sigma^2 t \sin \gamma} \frac{1}{s_1 s_2} \exp\left(-\frac{1}{2} \frac{L_1^2 - 2L_1 L_2 \cos \gamma + L_2^2}{\sigma^2 t \sin^2 \gamma}\right) p_\theta(\gamma) d\gamma \\
&= \int_0^\pi \exp(g(\gamma)) d\gamma \\
&= \int_0^\pi \exp\left(g(\gamma^*) + g'(\gamma^*)(\gamma - \gamma^*) + \frac{1}{2}g''(\gamma^*)(\gamma - \gamma^*)^2\right) d\gamma
\end{aligned}$$

Say γ^* is the value at which $g(\gamma)$ is maximised, then $g'(\gamma^*) = 0$, therefore,

$$\begin{aligned}
& \approx \int_0^\pi \exp\left(g(\gamma^*) + \frac{1}{2}g''(\gamma^*)(\gamma - \gamma^*)^2\right) d\gamma \\
&= \exp(g(\gamma^*)) \sqrt{\frac{2\pi}{-g''(\gamma^*)}} \left(\Phi\left(\sqrt{-g''(\gamma^*)}(\pi - \gamma^*)\right) - \Phi\left(-\sqrt{-g''(\gamma^*)}\gamma^*\right) \right)
\end{aligned}$$

To obtain γ^* solve $g'(\gamma) = 0$ and choose a γ^* such that $g''(\gamma^*) < 0$. □

Similarly we obtain the joint cumulative distribution function for the assets,

Corollary 2.1.1. *The joint cumulative distribution function of the asset values is given by,*

$$\mathbb{P}(S_{1,t} < y_1, S_{2,t} < y_2) \approx \exp(f(\gamma^*)) \sqrt{\frac{2\pi}{-f''(\gamma^*)}} \left(\Phi(\sqrt{-f''(\gamma^*)}(\pi - \gamma^*)) - \Phi(-\sqrt{-f''(\gamma^*)}\gamma^*) \right) \quad (3)$$

where $f(\gamma) = \log p_\theta(\gamma) + \log \Phi_2(c_1, c_2; \cos \gamma)$. Here Φ_2 is the cumulative distribution function of the standard bivariate normal distribution with correlation $\cos \gamma$, with $c_1 = \frac{\log y_1 - \mu}{\sigma}$ and $c_2 = \frac{\log y_2 - \mu}{\sigma}$.

2.2 First passage time distribution

We want to understand the distribution of the first time an asset defaults. Let,

$$\tau_i = \inf\{t > 0 : S_{i,t} < B_i\}, i = 1, 2$$

Let, $x_{i,t} = \log S_{i,t}$, and $x_{1,0} = \log S_{1,0}$ and $x_{2,0} = \log S_{2,0}$. Define,

$$\tau_i^* = \inf\{t > 0 : x_{i,t} < \log B_i\}, i = 1, 2$$

It then follows from the above theorem,

Theorem 2.2. *The joint density of the hitting times conditional on the correlation at time t , ρ_t , is given by,*

$$\begin{aligned} f(\tau_1^*, \tau_2^*; \rho)(t_1, t_2) &= \sum_{i=1}^2 \sum_{j=1; i \neq j}^2 \frac{\sqrt{2\pi}}{2\alpha^2 \sigma t_i \sqrt{(t_j - t_i)^3}} \exp \left(K_i(-\log B_i + x_{0i}) - K_j x_{0j} - \frac{\mu^* \log B_j}{\sigma^2} - K_i N_j t_i \right. \\ &\quad \left. - \frac{(\mu^*)^2 t_j}{2\sigma^2} \right) \int_{-\infty}^{-\log B_j} \exp(-K_i \rho x_j) \exp \left(-\frac{(\bar{r}_0)^2 + \sigma^2(-\log B_j + x_j)^2}{2t_i K_3^2} - \frac{(-\log B_j + x_j)^2}{2\sigma^2(t_j - t_i)} \right) \\ &\quad G_{ji}(\bar{r}_0, \phi_0, x_j, t_i) dx_j \end{aligned}$$

where,

$$\mu^* = -\left(\mu - \frac{1}{2}\sigma^2\right),$$

$$K_1 = \frac{\mu^*(1-\rho)}{\sigma^2(1-\rho^2)}, K_2 = \frac{\mu^*(1+\rho)}{\sigma^2(1-\rho^2)}, K_3 = \sigma^2 \sqrt{1-\rho^2},$$

$$\alpha = \arctan \left(-\frac{\sqrt{1-\rho^2}}{\rho} \right) \in (0, \pi),$$

$$\bar{r}_0 = \sqrt{\sigma^2(\log B_2 - x_{20})^2 + \sigma^2(\log B_1 - x_{10})^2 - 2\sigma^2\rho(-\log B_1 + x_{10})(-\log B_2 + x_{20})},$$

$$\phi_0 = \arctan \left(\frac{\sqrt{1-\rho^2}(-\log B_2 + x_{20})}{(-\log B_1 + x_{10}) - \rho(-\log B_2 + x_{20})} \right),$$

$$G_{ij}(\bar{r}_0, \phi_0, x_i, t) = \sum_{n=1}^{\infty} \delta_i n \sin\left(\frac{n\pi\phi_0}{\alpha}\right) I_{\frac{n\pi}{\alpha}}\left(\frac{\sigma_j(-\log B_i + x_i)\bar{r}_0}{K_3^2 t}\right), \delta_1 = 1, \delta_2 = (-1)^{n+1},$$

here I is the modified Bessel function of the first kind.

Proof. The result follows from Theorem 4 of Sacerdote et al., 2016. \square

The unconditional joint first passage time is given by,

Corollary 2.2.1.

$$\mathbb{P}(\tau_1 < t_1, \tau_2 < t_2) = \mathbb{E}[\mathbb{P}(\tau_1 < t_1, \tau_2 < t_2 | \rho_t)] \quad (4)$$

here the inner distribution will be calculated using Theorem 2.2.

To efficiently numerically evaluate the above probability we generate various paths of ρ_t and we evaluate $\mathbb{P}(\tau_1 < t_1, \tau_2 < t_2 | \rho_t)$, and take their sample means to obtain the unconditional joint first passage times.

2.3 Survival Probability

We aim to compute the joint survival probability

$$\mathbb{P}(S_1(t) > B_1, S_2(t) > B_2, \tau > t), \quad \tau = \min(\tau_1, \tau_2),$$

where τ_i is the first time borrower i hits its default barrier. A key ingredient is the killed transition density of an associated bivariate Wiener process. We record this technical result next.

Lemma 2.3. Let $X(t) = (X_1(t), X_2(t))^\top$ solve the bivariate Wiener SDE

$$dX(t) = \mu dt + L dW(t), \quad X(0) = x_0 = (x_{01}, x_{02})^\top,$$

where W is a two-dimensional standard Brownian motion,

$$\mu = \begin{pmatrix} \mu_1 \\ \mu_2 \end{pmatrix}, \quad L = \begin{pmatrix} \sigma_1 & 0 \\ \rho\sigma_2 & \sigma_2\sqrt{1-\rho^2} \end{pmatrix}, \quad \rho \in (-1, 1), \quad \sigma_1, \sigma_2 > 0.$$

Let the constant upper barriers B_1, B_2 satisfy $x_{0i} < B_i$ and define

$$\tau = \inf\{t > 0 : X_1(t) \geq B_1 \text{ or } X_2(t) \geq B_2\}, \quad D = (-\infty, B_1) \times (-\infty, B_2).$$

The killed transition density $f_X^a(\cdot, t | x_0)$ on D is defined by

$$\mathbb{P}(X(t) \in dx, \tau > t | X(0) = x_0) = f_X^a(x, t | x_0) dx, \quad x \in D, t > 0.$$

Then, for $x \in D$ and $t > 0$,

$$f_X^a(x, t | x_0) = \frac{2}{\alpha K_3 t} \exp\left(K_1(x_1 - x_{01}) + K_2(x_2 - x_{02}) - \lambda t - \frac{\bar{r}(x)^2 + \bar{r}_0^2}{2K_3^2 t}\right) H(\bar{r}(x), \bar{r}_0, \phi(x), \phi_0, t), \quad (5)$$

where the auxiliary quantities are as follows.

Let $\tilde{\Sigma} = LL^\top$ be the covariance matrix,

$$\tilde{\Sigma} = \begin{pmatrix} \sigma_1^2 & \rho\sigma_1\sigma_2 \\ \rho\sigma_1\sigma_2 & \sigma_2^2 \end{pmatrix}, \quad K = \tilde{\Sigma}^{-1}\mu = \begin{pmatrix} K_1 \\ K_2 \end{pmatrix}, \quad \lambda = \frac{1}{2}\mu^\top\tilde{\Sigma}^{-1}\mu.$$

Equivalently,

$$K_1 = \frac{\sigma_2\mu_1 - \rho\sigma_1\mu_2}{\sigma_1^2\sigma_2(1 - \rho^2)}, \quad K_2 = \frac{\sigma_1\mu_2 - \rho\sigma_2\mu_1}{\sigma_1\sigma_2^2(1 - \rho^2)}, \quad K_3 = \sigma_1\sigma_2\sqrt{1 - \rho^2},$$

and

$$\lambda = \frac{\sigma_1^2\mu_2^2 - 2\rho\sigma_1\sigma_2\mu_1\mu_2 + \sigma_2^2\mu_1^2}{2K_3^2}.$$

Define the wedge angle,

$$\alpha = \text{atan2}(\sqrt{1 - \rho^2}, -\rho) \in (0, \pi).$$

For $x \in D$ define $\bar{r}(x) > 0$ and $\phi(x) \in (0, \alpha)$ by

$$\begin{aligned} \bar{r}(x) &= \sqrt{\sigma_1^2(B_2 - x_2)^2 + \sigma_2^2(B_1 - x_1)^2 - 2\rho\sigma_1\sigma_2(B_1 - x_1)(B_2 - x_2)}, \\ \bar{r}(x) \cos \phi(x) &= \sigma_2(B_1 - x_1) - \rho\sigma_1(B_2 - x_2), \\ \bar{r}(x) \sin \phi(x) &= \sigma_1\sqrt{1 - \rho^2}(B_2 - x_2), \end{aligned}$$

and set $\bar{r}_0 = \bar{r}(x_0)$ and $\phi_0 = \phi(x_0)$.

$$H(\bar{r}, \bar{r}_0, \phi, \phi_0, t) = \sum_{n=1}^{\infty} \sin\left(\frac{n\pi\phi}{\alpha}\right) \sin\left(\frac{n\pi\phi_0}{\alpha}\right) I_{n\pi/\alpha}\left(\frac{\bar{r}\bar{r}_0}{K_3^2 t}\right),$$

where $I_\nu(\cdot)$ is the modified Bessel function of the first kind.

Proof. For $x \in D$ and $t > 0$, the killed density $f_X^a(\cdot, t | x_0)$ is the unique solution of the forward Kolmogorov equation on D with absorbing boundary conditions,

$$\partial_t f = \frac{\sigma_1^2}{2}\partial_{x_1x_1}f + \frac{\sigma_2^2}{2}\partial_{x_2x_2}f + \rho\sigma_1\sigma_2\partial_{x_1x_2}f - \mu_1\partial_{x_1}f - \mu_2\partial_{x_2}f, \quad x \in D, \quad t > 0, \quad (6)$$

$$\lim_{t \downarrow 0} f(x, t | x_0) = \delta(x_1 - x_{01})\delta(x_2 - x_{02}), \quad (7)$$

$$f(x, t | x_0)|_{x_1=B_1} = 0, \quad f(x, t | x_0)|_{x_2=B_2} = 0. \quad (8)$$

Let $K = \tilde{\Sigma}^{-1}\mu$ and $\lambda = \frac{1}{2}\mu^\top\tilde{\Sigma}^{-1}\mu$. Define

$$f(x, t | x_0) = \exp(K^\top(x - x_0) - \lambda t)g(x, t | x_0). \quad (9)$$

A direct substitution of (9) into (6) shows that the first-derivative terms cancel because $\tilde{\Sigma}K = \mu$, and the remaining zeroth-order term is canceled by the choice of λ . Consequently g solves the driftless equation,

$$\partial_t g = \frac{1}{2}\nabla^\top\tilde{\Sigma}\nabla g = \frac{\sigma_1^2}{2}\partial_{x_1x_1}g + \frac{\sigma_2^2}{2}\partial_{x_2x_2}g + \rho\sigma_1\sigma_2\partial_{x_1x_2}g, \quad x \in D, \quad t > 0, \quad (10)$$

with the same boundary conditions (8) and the same delta initial condition (7).

We introduce the distance-to-boundary variables $d_1 = B_1 - x_1$, $d_2 = B_2 - x_2$ and the linear map,

$$y_1 = \sigma_2 d_1 - \rho \sigma_1 d_2, \quad y_2 = \sigma_1 \sqrt{1 - \rho^2} d_2.$$

A direct computation gives $|\det(\partial y/\partial x)| = \sigma_1 \sigma_2 \sqrt{1 - \rho^2} = K_3$ and $(\partial y/\partial x) \widetilde{\Sigma} (\partial y/\partial x)^\top = K_3^2 I_2$, so (10) becomes a heat equation in the (y_1, y_2) variables with diffusion coefficient $K_3^2/2$. The strip D is mapped to a wedge of angle $\alpha \in (0, \pi)$. In polar coordinates (\bar{r}, ϕ) for y this yields $\bar{r}(x) = \sqrt{y_1^2 + y_2^2}$ and $\phi(x) = \text{atan2}(y_2, y_1) \in (0, \alpha)$.

The Dirichlet heat kernel in a wedge admits eigenfunction expansion in ϕ (see Lemma 1, Bañuelos and Smits, 1997), leading to the representation,

$$g(x, t | x_0) = \frac{2}{\alpha K_3 t} \exp\left(-\frac{\bar{r}(x)^2 + \bar{r}_0^2}{2K_3^2 t}\right) H(\bar{r}(x), \bar{r}_0, \phi(x), \phi_0, t),$$

where H is the Bessel-series given in the statement.

Multiplying the driftless kernel by the drift-removal factor yields (5). \square

We note that Lemma 2.3 corrects Lemma 2 of Sacerdote et al., 2016, where the term $\exp(K_1 x_1 + K_2 x_2)$ was absent in the expression presented.

It follows from Lemma 2.3 that the conditional survival probability is given by,

Theorem 2.4.

$$\begin{aligned} & \mathbb{P}(S_{1,t} > B_1, S_{2,t} > B_2, \tau > t | \rho_t) \\ &= \int_{-\infty}^{-\log B_2} \int_{-\infty}^{-\log B_1} \frac{2}{\alpha K_3 t} \exp\left(K_1(x_1 - x_{01}) + K_2(x_2 - x_{02}) - \lambda t - \frac{\bar{r}(x)^2 + \bar{r}_0^2}{2K_3^2 t}\right) \\ & H(\bar{r}(x), \bar{r}_0, \phi(x), \phi_0, t) dx_1 dx_2 \end{aligned} \quad (11)$$

where,

$$K_1 = \frac{\mu^*(1 - \rho_t)}{\sigma^2(1 - \rho_t^2)}, \quad K_2 = \frac{\mu^*(1 - \rho_t)}{\sigma^2(1 - \rho_t^2)}, \quad K_3 = \sigma^2 \sqrt{1 - \rho_t^2},$$

and

$$\lambda = \frac{2\sigma^2(\mu^*)^2(1 - \rho_t)}{2K_3^2}.$$

$$\alpha = \text{atan2}\left(\sqrt{1 - \rho_t^2}, -\rho\right) \in (0, \pi).$$

For $x \in D$ define $\bar{r}(x) > 0$ and $\phi(x) \in (0, \alpha)$ by

$$\begin{aligned} \bar{r}(x) &= \sqrt{\sigma^2(-\log B_2 + x_2)^2 + \sigma^2(-\log B_1 + x_1)^2 - 2\rho\sigma^2(-\log B_1 + x_1)(-\log B_2 + x_2)}, \\ \bar{r}(x) \cos \phi(x) &= \sigma((-\log B_1 + x_1) - \rho(-\log B_2 + x_2)), \end{aligned}$$

$$\bar{r}(x) \sin \phi(x) = \sigma \sqrt{1 - \rho^2} (-\log B_2 + x_2),$$

and set $\bar{r}_0 = \bar{r}(x_0)$ and $\phi_0 = \phi(x_0)$.

$$H(\bar{r}, \bar{r}_0, \phi, \phi_0, t) = \sum_{n=1}^{\infty} \sin\left(\frac{n\pi\phi}{\alpha}\right) \sin\left(\frac{n\pi\phi_0}{\alpha}\right) I_{n\pi/\alpha}\left(\frac{\bar{r}\bar{r}_0}{K_3^2 t}\right),$$

where $I_\nu(\cdot)$ is the modified Bessel function of the first kind.

Corollary 2.4.1. *The unconditional survival probability is given by,*

$$\mathbb{P}(S_{1,t} > B_1, S_{2,t} > B_2, \tau > t) = \mathbb{E}[\mathbb{P}(S_{1,t} > B_1, S_{2,t} > B_2, \tau > t | \rho_t)]$$

Just like in the first passage time distribution case this probability can be numerically evaluated by Monte Carlo simulation of paths of ρ_t , and for each simulated path of ρ_t we evaluate the above probability. The sample mean of all of these probabilities shall approximate the unconditional survival probability.

3 Simulation study

This section illustrates how stochastic correlation affects (i) joint default-at-horizon probabilities, (ii) joint survival probabilities, and (iii) joint first-passage (joint hitting) probabilities. Throughout, we keep the marginal asset dynamics fixed except for the parameter being varied, and we isolate the role of correlation dynamics by changing the von Mises parameters governing the angle diffusion θ_t and the induced correlation ρ_t .

3.1 Quantities of interest

We report three time-dependent objects for a two-name portfolio with default barriers (B_1, B_2) :

1. Joint default probability at horizon t :

$$p_{\text{JD}}(t) = \mathbb{P}(S_1(t) \leq B_1, S_2(t) \leq B_2).$$

This is a value-at-horizon joint default event.

2. Joint survival probability up to time t :

$$p_{\text{Surv}}(t) = \mathbb{P}(\tau_1 > t, \tau_2 > t), \quad \tau_i = \inf\{u > 0 : S_i(u) \leq B_i\}.$$

This is a path-dependent event and depends on the killed transition density described in Section 2.

3. Joint first-passage probability up to time t :

$$p_{\text{FPT}}(t) = \mathbb{P}(\tau_1 \leq t, \tau_2 \leq t).$$

This captures the likelihood of joint barrier crossing by time t .

3.2 Simulation design and numerical evaluation

We model dependence through a circular diffusion θ_t (von Mises process) and set $\rho_t = g(\theta_t)$, where g is chosen to ensure $\rho_t \in [0, 1]$ in the simulation design. For each time horizon t we generate N_ρ independent draws from the correlation distribution induced by θ_t , and then average conditional quantities over these draws:

$$\hat{p}(t) = \frac{1}{N_\rho} \sum_{m=1}^{N_\rho} p(t | \rho_t^{(m)}).$$

For the joint survival probability, $p(t | \rho)$ is evaluated by numerically integrating the killed density over the pre-default domain, using a truncated eigenfunction expansion and quadrature. For the joint first-passage probability, $p_{\text{FPT}}(t | \rho)$ is evaluated using the closed/semi-closed form joint hitting-time density from Section 2, integrated over a two-dimensional time grid; the computation is implemented in C++ for speed. The joint default-at-horizon probability is evaluated from the semi-closed form expression derived for the joint distribution of asset values (Section 2), with the remaining one-dimensional integral over the correlation state evaluated numerically.

Unless otherwise stated, we fix the barrier and initial levels $(B_1, B_2, S_1(0), S_2(0))$ and a baseline set of parameters for the asset and correlation dynamics, and then vary one parameter at a time. Time is measured in years and we evaluate $t \in \{0.1, 0.2, \dots, 1.1\}$.

3.3 Sensitivity to marginal asset volatility

Figure 1 shows that increasing the GBM volatility σ produces a substantial increase in the joint default-at-horizon probability across all maturities. The effect is strongest at short horizons: the joint default probability rises rapidly between $t = 0.1$ and $t \approx 0.4$, after which the curves flatten, indicating a saturation of incremental joint default risk over longer horizons.

The corresponding survival curves in Figure 2 are monotone decreasing in t as expected, and display clear separation across volatility levels. Higher σ accelerates barrier crossing and leads to markedly lower joint survival probabilities at every horizon. For example, the survival probability remains high for small σ even at $t \approx 1$, whereas it decays sharply for larger σ , reflecting the dominant role of marginal dispersion in path-dependent default events.

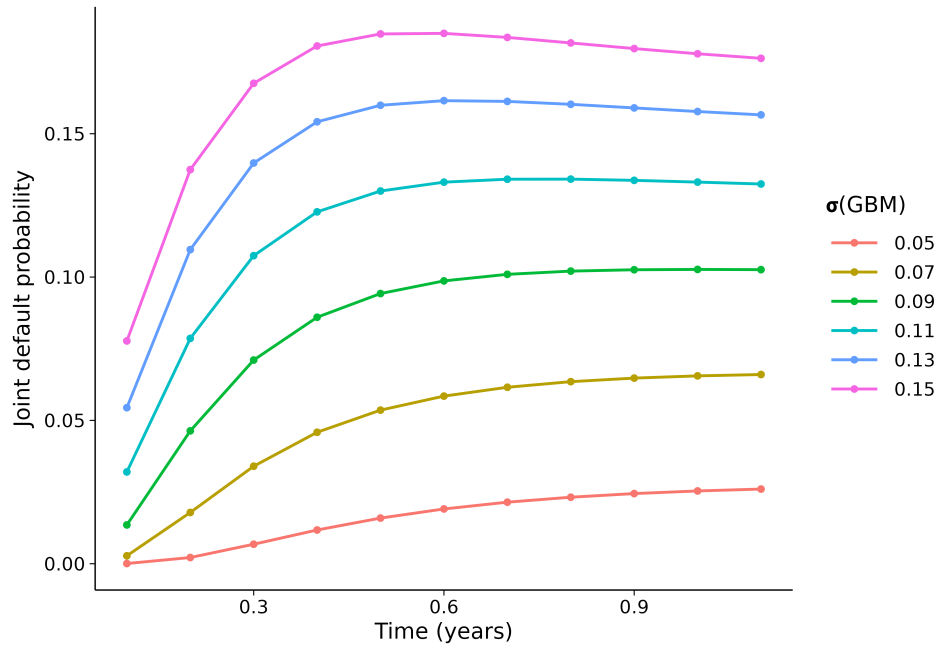


Figure 1: Joint default probability $p_{\text{JD}}(t)$ as a function of maturity t for varying GBM volatility σ . Higher marginal volatility increases joint default risk and leads to earlier saturation in t .

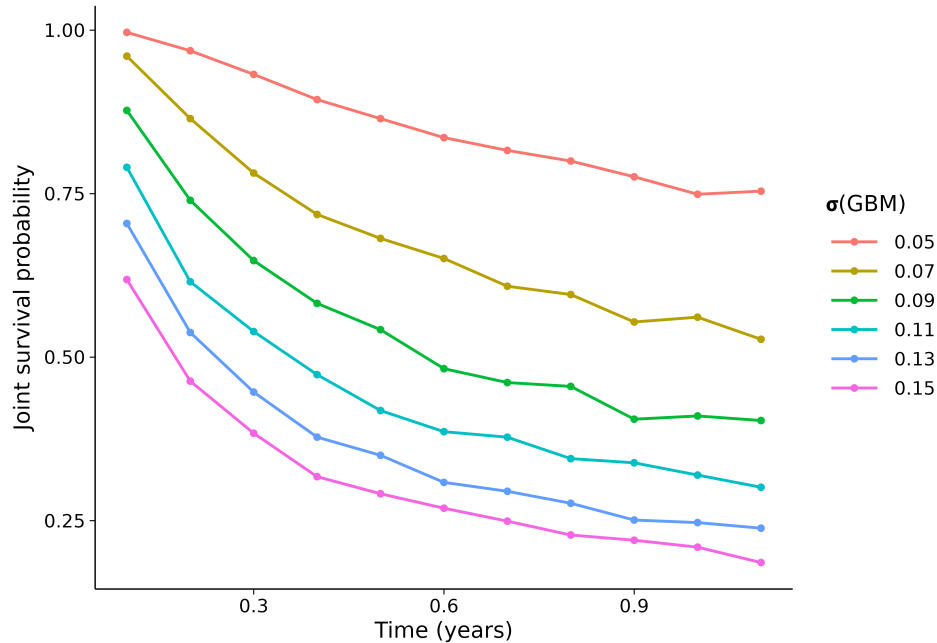


Figure 2: Joint survival probability $p_{\text{Surv}}(t) = \mathbb{P}(\tau_1 > t, \tau_2 > t)$ for varying GBM volatility σ . Survival decays faster and to lower levels as marginal volatility increases.

3.4 Sensitivity to correlation dynamics: volatility and persistence

Figures 3 and 4 isolate the role of stochastic correlation dynamics. In Figure 3, increasing the correlation volatility parameter σ_{von} lowers the joint default-at-horizon probability. Intuitively, larger σ_{von} induces greater dispersion in the correlation state over the horizon, weakening persistent clustering and reducing the effective average dependence relevant for joint default at a fixed time.

In contrast, Figure 4 shows that increasing the mean-reversion speed λ increases joint default risk across maturities. Stronger mean reversion concentrates the correlation state more tightly around its long-run mean, producing a more persistent dependence regime and therefore larger default clustering.

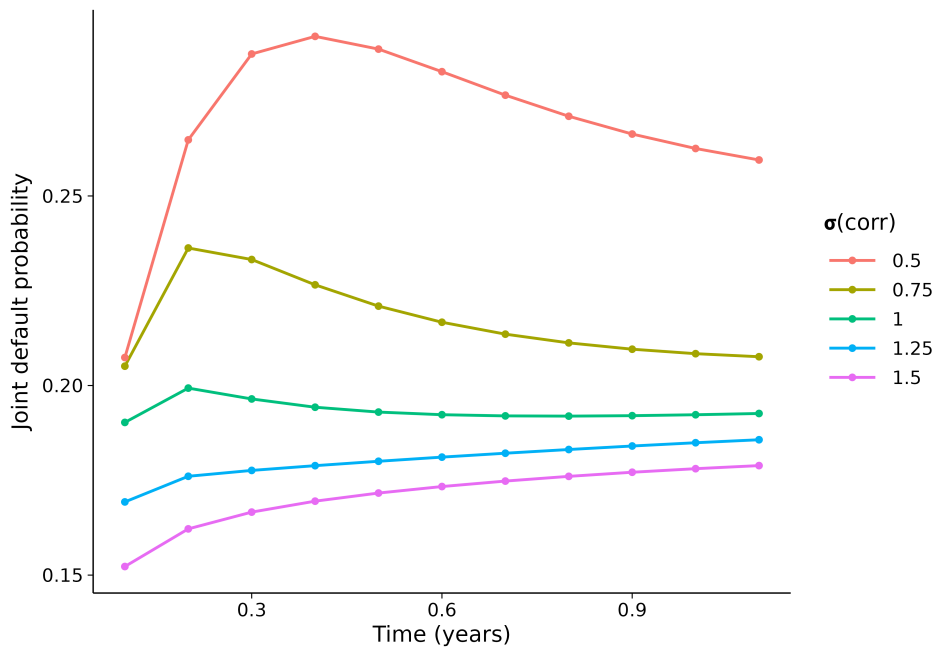


Figure 3: Joint default probability $p_{\text{JD}}(t)$ for varying correlation-volatility parameter σ_{von} in the von Mises correlation model. Higher σ_{von} reduces the level of joint default probabilities.

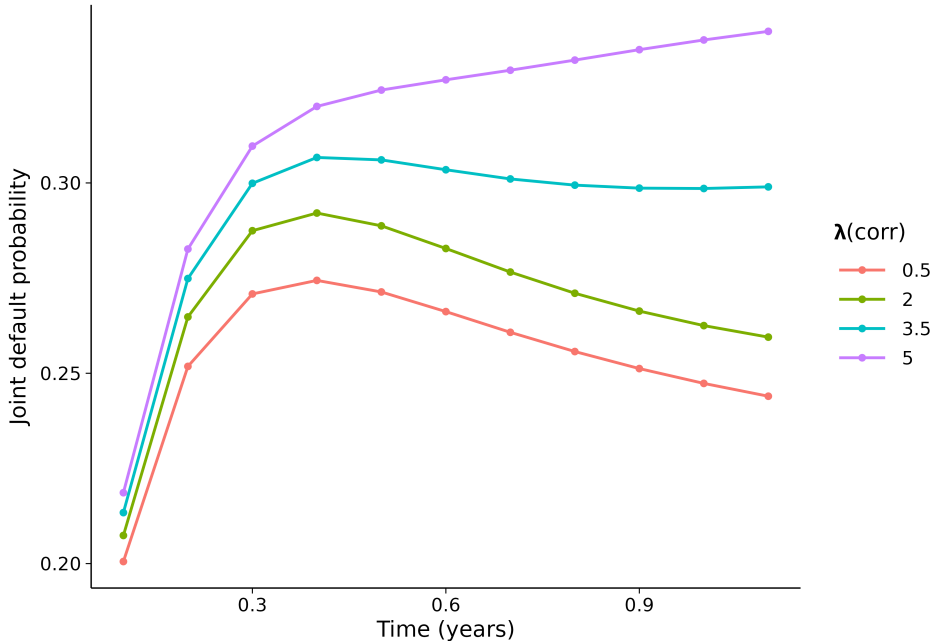


Figure 4: Joint default probability $p_{JD}(t)$ for varying mean-reversion speed λ of the correlation dynamics. Higher λ increases the level of joint default probabilities, consistent with more persistent dependence.

3.5 First-passage probabilities and joint barrier-crossing

Finally, Figures 5 and 6 report the joint first-passage probabilities. The dominant effect of marginal volatility persists: increasing the GBM volatility produces a sharp increase in joint first-passage likelihood at short horizons (Figure 5). We also observe a clear dependence effect: increasing the mean reversion parameter λ raises the joint first-passage probability (Figure 6), reflecting increased clustering when the correlation state is more persistent.

Because $p_{FPT}(t)$ is computed via a two-dimensional numerical integration together with Monte Carlo averaging over ρ_t draws, minor non-monotonicity in t can occur for a fixed grid resolution. The qualitative comparative statics across parameter values, however, are stable: higher marginal volatility and stronger correlation persistence both increase the likelihood of joint barrier crossing.

Tables 1–2 summarise the joint first-passage probability $p_{FPT}(t) = \mathbb{P}(\tau_1 \leq t, \tau_2 \leq t)$ at selected horizons. The dominant effect is marginal dispersion: increasing the GBM volatility from $\sigma = 0.05$ to $\sigma = 0.15$ raises $p_{FPT}(0.2)$ from 0.027 to 0.384 and increases $p_{FPT}(1.0)$ from 0.025 to 0.148, highlighting the strong sensitivity of joint barrier-crossing risk to asset volatility. Correlation dynamics also matter: varying the mean-reversion speed λ changes short-horizon joint first-passage probabilities noticeably (e.g., $p_{FPT}(0.2)$ increases from 0.349 at $\lambda = 0.5$ to about 0.415–0.418 for $\lambda \in \{3.5, 5\}$), while at longer horizons the ordering becomes less monotone and the spread narrows. This pattern is consistent with the fact that $p_{FPT}(t)$ depends on both the evolving correlation state and a two-dimensional time integration, so correlation persistence has its clearest impact on short-horizon joint crossing behaviour.

Table 3 reports sensitivity of the joint first-passage probability to the correlation-volatility parameter σ_{von} . Unlike the marginal volatility effect in Table 1, the impact of σ_{von} is not monotone across horizons: at $t = 0.2$ the joint crossing probability ranges from 0.287 to 0.398 across the values considered, while at $t = 0.6$ it ranges from 0.143 to 0.244. This non-monotonicity is economically plausible in a stochastic-correlation setting because increasing σ_{von} changes the entire distribution of the correlation state over $[0, t]$ (not just its mean), and $p_{\text{FPT}}(t)$ depends on both the induced dependence and the two-dimensional time integration used to aggregate the joint hitting-time density. Overall, the table shows that correlation volatility can shift joint first-passage likelihood materially even when marginal asset parameters are held fixed, reinforcing that correlation risk is a quantitatively relevant driver of joint tail events.

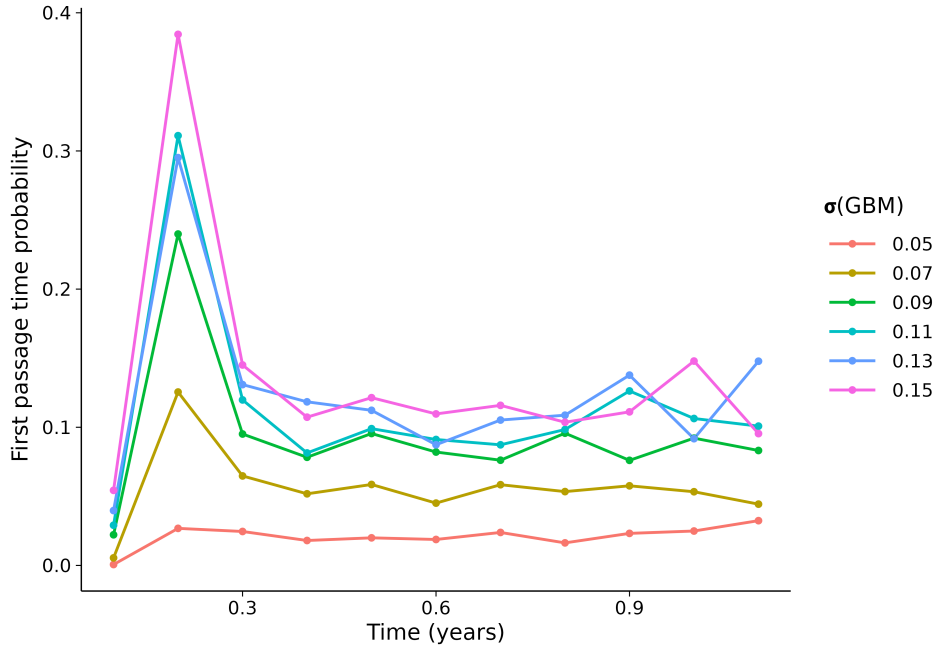


Figure 5: Joint first-passage probability $p_{\text{FPT}}(t) = \mathbb{P}(\tau_1 \leq t, \tau_2 \leq t)$ for varying GBM volatility σ . Higher volatility substantially increases short-horizon joint barrier-crossing likelihood.

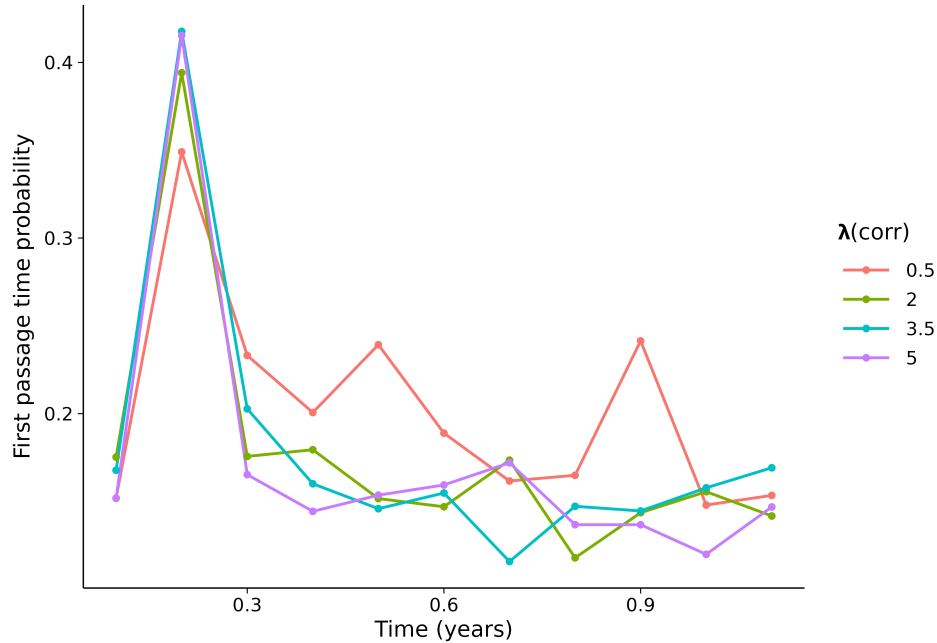


Figure 6: Joint first-passage probability $p_{\text{FPT}}(t)$ for varying mean-reversion speed λ in the correlation dynamics. Higher λ increases joint barrier-crossing likelihood, consistent with stronger default clustering.

Table 1: Joint first-passage probability $p_{\text{FPT}}(t) = \mathbb{P}(\tau_1 \leq t, \tau_2 \leq t)$ for varying GBM volatility σ (other parameters at baseline).

σ	$t = 0.2$	$t = 0.6$	$t = 1.0$
0.05	0.027	0.019	0.025
0.07	0.126	0.045	0.053
0.09	0.240	0.082	0.092
0.11	0.311	0.091	0.106
0.13	0.295	0.087	0.092
0.15	0.384	0.110	0.148

Table 2: Joint first-passage probability $p_{\text{FPT}}(t)$ for varying correlation mean-reversion speed λ in the von Mises correlation model (other parameters at baseline).

λ	$t = 0.2$	$t = 0.6$	$t = 1.0$
0.5	0.349	0.189	0.148
2.0	0.394	0.147	0.156
3.5	0.418	0.155	0.158
5.0	0.415	0.159	0.120

Table 3: Joint first-passage probability $p_{\text{FFPT}}(t) = \mathbb{P}(\tau_1 \leq t, \tau_2 \leq t)$ for varying correlation volatility σ_{von} in the von Mises correlation model (other parameters at baseline).

σ_{von}	$t = 0.2$	$t = 0.6$	$t = 1.0$
0.50	0.385	0.143	0.144
0.75	0.362	0.157	0.159
1.00	0.398	0.244	0.128
1.25	0.300	0.155	0.163
1.50	0.287	0.214	0.191

Across all three probability objects, the simulations highlight two robust messages. First, marginal dispersion (GBM volatility) strongly controls both value-at-horizon joint default risk and path-dependent survival/first-passage risk. Second, stochastic correlation dynamics materially change joint tail-event probabilities even when marginal dynamics are held fixed: increasing correlation volatility reduces joint default clustering, while increasing correlation persistence increases clustering. These comparative statics provide quantitative evidence that correlation risk affects joint default and survival calculations in a manner consistent with the regulatory sensitivity of Vasicek-type capital formulas.

4 Empirical illustration: U.S. bank charge-off data

4.1 Data

We use the Federal Reserve Board release *Charge-Off and Delinquency Rates on Loans and Leases at Commercial Banks* to obtain quarterly *net charge-off rates* for a set of major loan categories.¹ This dataset has been previously analyzed in the context of credit risk modelling in the literature, for e.g. see Metzler, 2020. Charge-offs are not identical to defaults, they reflect accounting conventions, timing of recognition, and recoveries; but they provide a long and consistently defined macro-credit time series capturing realised credit deterioration within each category. Accordingly, we treat the charge-off rate as a reduced-form proxy for a portfolio default rate at the quarterly frequency.

Let $\{c_t\}_{t=1}^T$ denote the observed quarterly net charge-off rate in a given category, expressed as a fraction in $(0, 1)$. Our empirical objective is to infer a time-varying effective dependence index ρ_t that is consistent with a Vasicek interpretation of default clustering. We then illustrate how this stochastic dependence, when fed into the model developed in Section 2, changes joint default-at-horizon, joint survival, and joint first-passage probabilities.

4.2 Estimation

In the Vasicek large-pool limit, the portfolio default rate has a closed-form distribution conditional on an unconditional default probability p and an asset-correlation param-

¹Data source: <https://www.federalreserve.gov/releases/chargeoff/>.

eter ρ . We use this distribution as an observation model for the charge-off series.

For each category we set the long-run default proxy as the sample mean

$$p \equiv \bar{c} = \frac{1}{T} \sum_{t=1}^T c_t,$$

and treat each c_t as a draw from the Vasicek density conditional on ρ_t . Let $z_t = \Phi^{-1}(c_t)$ and $z_p = \Phi^{-1}(p)$. Then the Vasicek density can be written in the convenient exponential form

$$f_{\text{Vas}}(c_t | \rho_t, p) = \sqrt{\frac{1-\rho_t}{\rho_t}} \exp\left(-\frac{(\sqrt{1-\rho_t}z_t - z_p)^2}{2\rho_t} + \frac{1}{2}z_t^2\right), \quad c_t \in (0, 1), \rho_t \in (0, 1),$$

which is equivalent to the familiar ratio representation $f_{\text{Vas}}(c | \rho, p) = \frac{\sqrt{1-\rho} \phi((\sqrt{1-\rho}z - z_p)/\sqrt{\rho})}{\sqrt{\rho} \phi(z)}$ with $z = \Phi^{-1}(c)$. The corresponding log-likelihood contribution is

$$\ell_{\text{Vas}}(c_t; \rho_t, p) = \frac{1}{2} \log\left(\frac{1-\rho_t}{\rho_t}\right) - \frac{(\sqrt{1-\rho_t}z_t - z_p)^2}{2\rho_t} + \frac{1}{2}z_t^2.$$

Economically, this likelihood prefers larger ρ_t in periods where the realised default proxy exhibits unusually high outcomes (large z_t) relative to the long-run level p , because higher correlation increases the probability mass in the upper tail of the Vasicek distribution.

Credit-portfolio dependence is typically nonnegative at the ASRF level, and we enforce $\rho_t \in (0, 1)$ by construction. To connect with the geometric identity $\rho = \cos^2 \theta$ (Section 2) while restricting to nonnegative dependence, we use the parameterisation

$$\rho_t = \cos^2(\varphi_t), \varphi_t \in (0, \pi/2), \varphi_t = \arccos(\sqrt{\rho_t}).$$

This mapping has Jacobian

$$\left| \frac{d\varphi_t}{d\rho_t} \right| = \frac{1}{2\sqrt{\rho_t(1-\rho_t)}},$$

which must be included when we optimise over ρ_t but impose dynamics on φ_t .

We consider the von Mises process for modelling φ_t . The transition density of the von Mises process is available in closed form (see Majumdar and Laha, 2024), enabling likelihood-based inference.

For each loan category we estimate the entire latent dependence path $\rho_{1:T}$ jointly with diffusion parameters by penalised maximum likelihood. Let $\psi = (\lambda, \sigma, \mu)$ for von Mises process and $\psi = (\sigma_{\text{cbm}})$ for CBM. We maximise

$$\max_{\rho_{1:T}, \psi} \sum_{t=1}^T \ell_{\text{Vas}}(c_t; \rho_t, p) + \sum_{t=2}^T \log p_\psi(\varphi_t | \varphi_{t-1}) + \sum_{t=1}^T \log \left| \frac{d\varphi_t}{d\rho_t} \right| - \eta \sum_{t=2}^T (\rho_t - \rho_{t-1})^2 - \pi(\psi), \quad (12)$$

where $p_\psi(\varphi_t | \varphi_{t-1})$ denotes the transition density of the chosen circular diffusion and the roughness penalty stabilises the inferred path when the data are only weakly

informative about ρ_t . The penalty $\pi(\psi)$ represents mild regularisation on diffusion parameters (used only to prevent implausible boundary solutions).

We solve (12) using box-constrained L-BFGS-B, directly optimising over $(\rho_{1:T}, \psi)$. To avoid numerical singularities in the Jacobian and in the Vasicek likelihood near $\rho = 0$ or $\rho = 1$, we constrain

$$\rho_t \in [0.01, 0.99], \quad \lambda \in [1, 10], \quad \sigma \in [0.5, 5], \quad \mu \in [0, \pi/2],$$

and evaluate transitions at the quarterly step size (i.e., $\Delta t = 1$ quarter, equivalently $\Delta t = 0.25$ years under a year time unit).²

The inferred series $\hat{\rho}_t$ should be interpreted as an effective ASRF dependence index inferred from portfolio-level default proxies. It is not a firm-level equity correlation or a micro-level pairwise asset correlation. Rather, it is the time-varying dependence parameter that makes the Vasicek large-pool distribution consistent with the observed dispersion and clustering of category-level credit outcomes. This is precisely the dependence object that drives joint tail-event probabilities in Vasicek credit risk calculations.

Figures 7–9 plot $\hat{\rho}_t$ under the von Mises process specification for representative categories, and Table 4 summarises the implied dependence levels. Three stylised facts stand out.

Across categories, $\hat{\rho}_t$ is far from constant: dependence exhibits low-correlation regimes punctuated by episodes of elevated correlation. In an ASRF interpretation, these spikes correspond to periods in which a larger share of realised credit deterioration is explained by a common systematic driver rather than category-specific noise. From a tail-risk perspective, this regime switching is the empirical analogue of correlation risk: joint-event probabilities are effectively mixtures over dependence states rather than being governed by a single constant ρ .

Real-estate-related categories exhibit materially higher inferred dependence than consumer categories. Table 4 shows that real-estate categories have upper-tail dependence (e.g., the 95th percentile of $\hat{\rho}_t$) that is several times their typical mean, indicating pronounced clustering under stress. In contrast, consumer categories (including credit cards) spend a large fraction of quarters at the lower bound $\rho_t = 0.01$. A natural interpretation is that within-category charge-off variation for consumer credit is often dominated by idiosyncratic/category-specific effects, while real-estate portfolios exhibit more pronounced common-factor comovement in loss outcomes.

For the von Mises process model we report the concentration index

$$\hat{\kappa} = \frac{2\hat{\lambda}}{\hat{\sigma}^2},$$

which measures mean-reversion strength relative to diffusion noise. Larger $\hat{\kappa}$ corresponds to a dependence state that is more tightly anchored around its long-run mean (fewer large excursions), whereas small $\hat{\kappa}$ corresponds to a more weakly anchored dependence state. In several categories the likelihood pushes diffusion parameters toward imposed bounds, indicating limited separate identification of (λ, σ, μ) from a single default-rate proxy. In such cases, the economically meaningful object is the inferred path $\hat{\rho}_t$ and its distributional summaries (mean and upper-tail), rather than the individual diffusion parameters.

²If any c_t values are reported as 0 due to rounding c_t , one may replace them by a small ε to ensure that $z_t = \Phi^{-1}(c_t)$ is finite; this affects only boundary observations and does not materially change inference.

Table 4: Summary of inferred dependence under the von Mises process model: mean, 95th percentile, maximum of $\hat{\rho}_t$, fraction of quarters at the lower bound (0.01), and $\hat{\kappa} = 2\hat{\lambda}/\hat{\sigma}^2$.

Category	mean($\hat{\rho}$)	q _{0.95} ($\hat{\rho}$)	max($\hat{\rho}$)	% at 0.01	$\hat{\kappa}$
Agricultural loans	0.070	0.256	0.407	28.2%	0.186
All consumer	0.018	0.060	0.108	68.7%	0.080
All real estate	0.093	0.301	0.366	21.5%	0.125
C&I loans	0.040	0.105	0.156	23.9%	0.080
Commercial real estate	0.123	0.304	0.367	15.8%	0.218
Credit cards	0.017	0.066	0.107	70.6%	0.080
Farmland	0.043	0.129	0.138	38.1%	0.771
Leases	0.039	0.126	0.278	36.8%	0.080
Other consumer	0.017	0.054	0.104	73.6%	0.080
Residential real estate	0.070	0.226	0.296	28.1%	1.188
Total loans & leases	0.024	0.096	0.117	48.5%	0.080

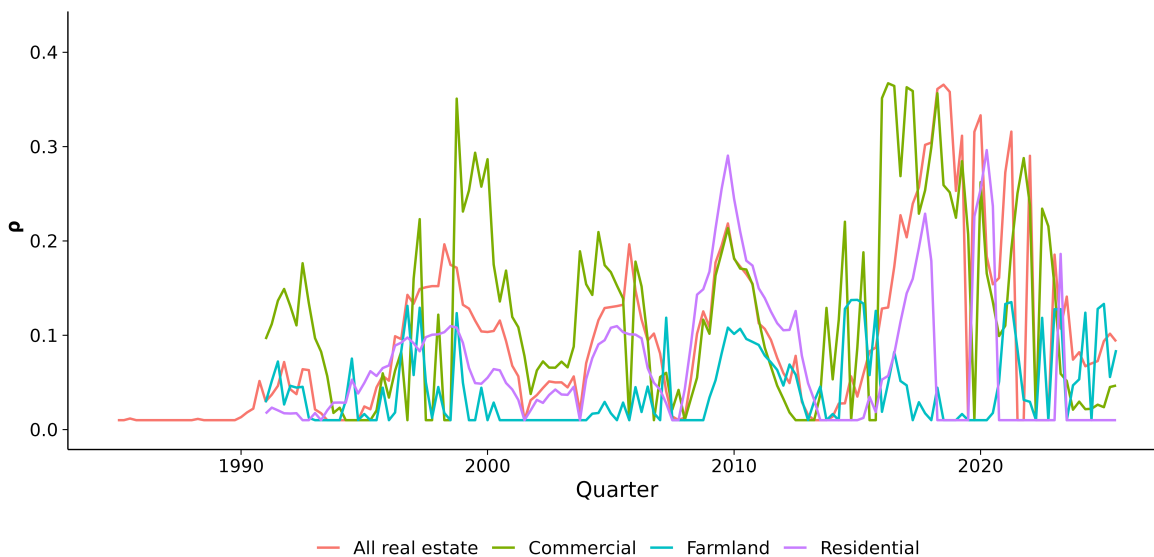


Figure 7: Estimated dependence paths $\hat{\rho}_t$ for selected real-estate categories.

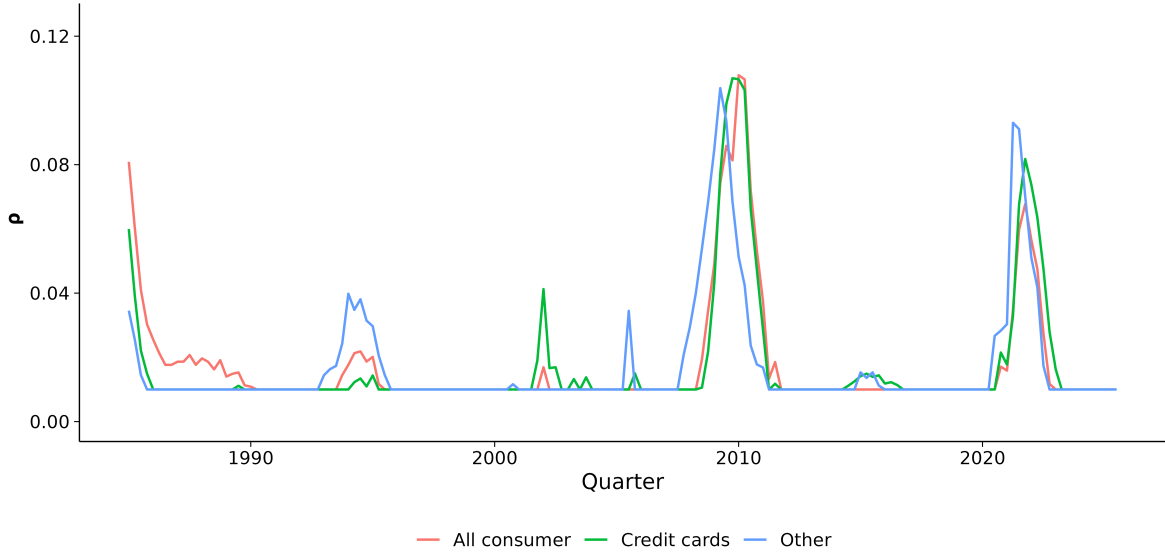


Figure 8: Estimated dependence paths $\hat{\rho}_t$ for consumer credit categories.

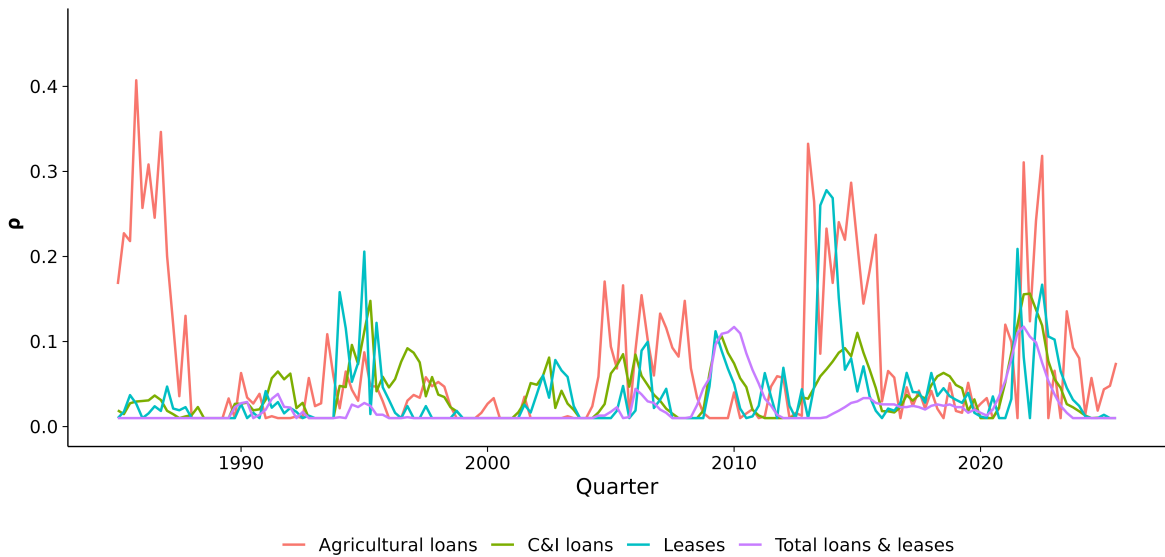


Figure 9: Estimated dependence paths $\hat{\rho}_t$ for agricultural loans, C&I loans, leases, and total loans and leases.

4.3 Distance-to-default calibration

To connect the empirical default-rate level to the barrier formulation in Section 2, we calibrate a category-specific distance-to-default (DD) from the long-run mean default proxy. Under GBM asset dynamics,

$$\mathbb{P}(S_T \leq B) = \Phi \left(\frac{\log(B/S_0) - (\mu - \frac{1}{2}\sigma^2)T}{\sigma\sqrt{T}} \right).$$

Setting the target one-horizon probability to $\bar{p} = \bar{c}$ yields the inversion

$$\text{DD} = -\Phi^{-1}(\bar{p}), \quad \log\left(\frac{S_0}{B}\right) = \text{DD}\sigma\sqrt{T} - \left(\mu - \frac{1}{2}\sigma^2\right)T.$$

We normalise $B = 100$ so that S_0 directly encodes the implied leverage ratio S_0/B . This calibration is not meant to assert that a category-level charge-off series literally arises from a single GBM firm; rather, it provides an interpretable structural normalisation that allows us to evaluate joint default, survival, and first-passage probabilities using the analytical machinery developed earlier.

4.4 Joint tail-event probabilities

Using the calibrated (S_0, B) together with the fitted von Mises process based correlation path, we compute three probability objects at horizon $T = 2$ years:

$$p_{\text{JD}}(T) = \mathbb{P}(S_1(T) \leq B_1, S_2(T) \leq B_2), p_{\text{Surv}}(T) = \mathbb{P}(\tau_1 > T, \tau_2 > T), p_{\text{FPT}}(T) = \mathbb{P}(\tau_1 \leq T, \tau_2 \leq T).$$

Conditional on a fixed correlation level ρ , these quantities are evaluated using the closed/semi-closed formulas in Section 2. To incorporate correlation risk in a transparent and computationally efficient way, we adopt a terminal-mixture approximation: we simulate ρ_T under the fitted dependence diffusion and average the conditional probabilities,

$$\hat{p}(T) = \frac{1}{N_\rho} \sum_{m=1}^{N_\rho} p(T | \rho_T^{(m)}).$$

This approach isolates the effect of uncertainty in the dependence state over horizon T while preserving the analytic conditional structure. A fully pathwise treatment (where correlation varies continuously inside the barrier events) would require integrating over correlation paths; we view that extension as natural but beyond the scope of this illustration.

Forecasting results and interpretation. Table 5 reports the calibrated DD, the von Mises concentration index $\hat{\kappa}$, and the three probability measures at $T = 2$ years. Two economic drivers are visible in the cross section:

- **Marginal credit quality (DD).** Lower DD corresponds to higher marginal default risk and therefore mechanically increases joint default and joint barrier-crossing probabilities. Consumer credit (especially credit cards) exhibits the lowest DD and correspondingly the highest joint default and first-passage probabilities, together with the lowest survival probability.
- **Systematic clustering (dependence).** Categories with higher inferred dependence (notably real-estate-related series) exhibit stronger joint-event likelihoods for a given DD. In these categories, the upper-tail behaviour of $\hat{\rho}_t$ (Table 4) implies the existence of stressed dependence regimes in which joint tail-event probabilities can be materially higher than what would be implied by a single “average” correlation input.

Table 5: Empirical forecasts at horizon $T = 2$ years using the von Mises process dependence model: calibrated distance-to-default (DD), joint default probability $p_{\text{JD}}(T)$, joint survival probability $p_{\text{Surv}}(T)$, joint first-passage probability $p_{\text{FPT}}(T)$, and $\hat{\kappa}$.

Category	DD	$p_{\text{JD}}(T)$	$p_{\text{Surv}}(T)$	$p_{\text{FPT}}(T)$	$\hat{\kappa}$
All real estate loans	2.640	0.0316	0.6032	0.0279	0.1252
Residential real estate	2.690	0.0231	0.6148	0.0279	1.1884
Commercial real estate	2.601	0.0320	0.6073	0.0283	0.2176
Farmland loans	3.103	0.0175	0.6992	0.0166	0.7707
All consumer loans	1.984	0.0517	0.4338	0.0602	0.0800
Credit card loans	1.721	0.0612	0.3633	0.0771	0.0800
Other consumer loans	2.302	0.0408	0.5253	0.0410	0.0800
Leases	2.639	0.0323	0.5963	0.0307	0.0800
C&I loans	2.429	0.0372	0.5549	0.0362	0.0800
Agricultural loans	2.614	0.0317	0.6077	0.0271	0.1858
Total loans & leases	2.381	0.0387	0.5439	0.0379	0.0800

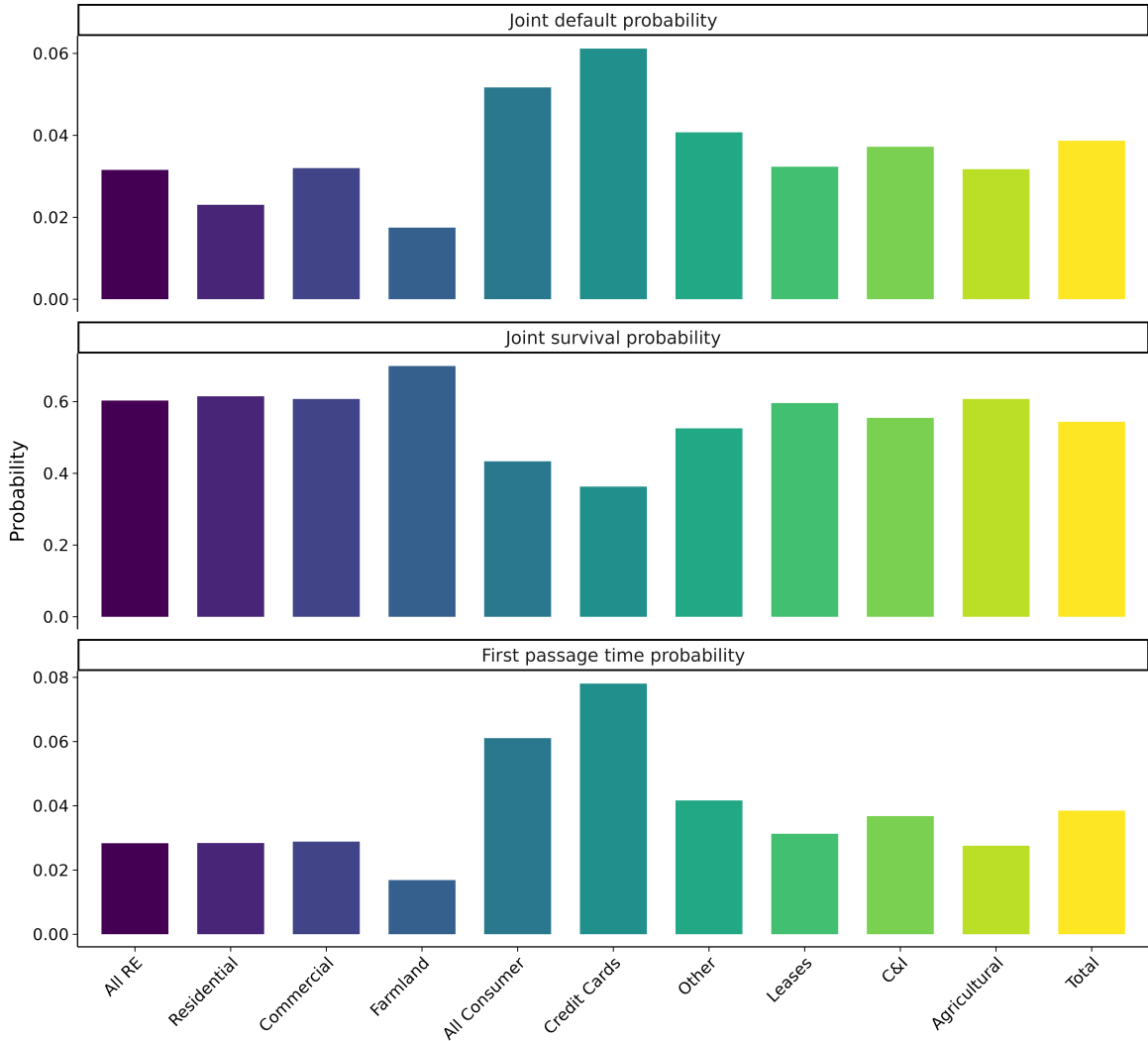


Figure 10: Empirical probability summaries at horizon $T = 2$ years by loan category: joint default, joint survival, and joint first-passage probabilities under the von Mises process dependence model.

Three caveats are important. First, charge-offs are an imperfect proxy for defaults and incorporate recoveries and accounting timing; therefore $\hat{\rho}_t$ should be interpreted as a dependence index for realised credit-loss outcomes rather than a structural firm-default correlation. Second, $\hat{\rho}_t$ is inferred at the category level under a large-pool approximation; it does not identify micro-level pairwise firm correlations nor cross-category dependence. Third, diffusion parameters can be weakly identified from a single default-proxy time series and may be influenced by constraints; for this reason the focus is on the inferred dependence path and its upper-tail behaviour rather than over-interpreting individual parameter values. Finally, the terminal-mixture forecasting step integrates out uncertainty in ρ_T while evaluating conditional joint events under a fixed correlation state; this is a transparent and tractable approximation aligned with our conditional formulas, but it is not identical to a fully pathwise stochastic-correlation model inside the barrier events.

5 Conclusion

This paper develops a stochastic-correlation extension of the Vasicek credit risk model aimed at capturing correlation risk while preserving analytical and computational tractability. In the classical Vasicek setting, dependence is summarised by a single constant asset-correlation parameter, yet empirical credit dependence is well known to be time-varying and typically stronger during stress. Because correlation directly controls default clustering, uncertainty and dynamics in correlation naturally translate into uncertainty and dynamics in joint tail-event probabilities.

Our main modelling contribution is to represent the correlation state through a bounded geometric mapping, $\rho_t = \cos(\theta_t)$ (and, when restricting to nonnegative dependence, $\rho_t = \cos^2(\varphi_t)$), where the angle evolves as a diffusion on the circle. This construction enforces admissible bounds by design and enables the use of circular diffusions with tractable transition densities, including circular Brownian motion and mean-reverting von Mises dynamics. The resulting framework yields an operational “mixture” interpretation: conditional credit quantities are computed under a fixed dependence state and then averaged over the distribution induced by the stochastic correlation process.

On the analytical side, we derive building blocks needed for joint credit calculations under stochastic correlation. First, we obtain the joint distribution of two asset values as an explicit mixture over the correlation state and provide a Laplace approximation that reduces the remaining integration to a one-dimensional optimisation and curvature evaluation. Second, we characterise joint first-passage behaviour using known joint hitting-time results for correlated Wiener processes. Third, we express joint survival probabilities via a killed transition density in a wedge domain and record a corrected drift-dependent prefactor relative to earlier expressions. Together, these results provide a coherent set of conditional joint default, survival, and joint barrier-crossing objects that can be combined with stochastic dependence through Monte Carlo averaging or numerical quadrature over the correlation state.

The simulation study highlights two economically interpretable messages. Marginal asset dispersion (GBM volatility) remains a dominant driver of both value-at-horizon joint default risk and path-dependent joint survival/first-passage risk. Beyond this, stochastic correlation parameters materially affect joint tail events: stronger dependence persistence (higher mean reversion strength in the von Mises specification) increases joint default clustering and raises joint barrier-crossing likelihoods, while higher correlation volatility can reduce joint default-at-horizon probabilities by dispersing the dependence state and weakening sustained clustering. For joint first-passage events, the effect of correlation volatility need not be monotone because barrier-crossing probabilities depend on the entire dependence distribution and on time aggregation of the joint hitting-time density, not solely on average correlation.

Our empirical illustration uses U.S. bank charge-off rates as a long, consistently defined proxy for category-level credit deterioration and infers a time-varying effective ASRF dependence index. The estimates show pronounced time variation and substantial heterogeneity across categories: real-estate-related categories exhibit higher and more episodic dependence regimes, whereas consumer categories frequently imply very low effective dependence. Translating the inferred dependence dynamics into joint default, joint survival, and joint first-passage probabilities at a multi-year horizon illustrates that correlation risk can meaningfully shift joint tail-event likelihoods even

when marginal calibration is held fixed.

Several limitations suggest natural extensions. The analytical results in this paper focus on two-name joint objects and incorporate stochastic dependence primarily through averaging over the correlation state. A fully pathwise treatment in which correlation varies continuously inside the barrier events would require integrating over correlation paths and is a promising direction for future work. Extending the framework to multi-name portfolios and to portfolio loss distributions (including granularity and concentration effects) would further connect the model to regulatory capital and portfolio credit VaR applications. On the empirical side, charge-offs are an imperfect proxy for defaults and incorporate recoveries and accounting conventions; richer datasets (e.g., default and migration histories, or tranche-implied dependence information) could sharpen identification of dependence dynamics and enable more direct calibration of stochastic correlation parameters.

Overall, circular diffusion models provide a parsimonious, bounded, and tractable mechanism for introducing stochastic correlation into Vasicek-style credit risk calculations. By retaining closed or semi-closed conditional formulas and integrating correlation risk through an explicit mixture over dependence states, the framework offers a practical route to stress-sensitive joint default and survival analysis in structural credit risk settings.

Disclosure Statement

The opinions expressed in this work are solely those of the authors and do not represent in any way those of their current and past employers. No potential conflict of interest was reported by the authors.

Funding Declaration

No funding was received

References

- Andersen, L., & Sidenius, J. (2004). Extensions to the gaussian copula: Random recovery and random factor loadings. *Journal of Credit Risk Volume*, 1(1), 05.
- Asai, M., & McAleer, M. (2009). The structure of dynamic correlations in multivariate stochastic volatility models. *Journal of Econometrics*, 150(2), 182–192.
- Bakshi, G., Gao, X., & Zhong, Z. (2022). Decoding default risk: A review of modeling approaches, findings, and estimation methods. *Annual Review of Financial Economics*, 14(1), 391–413.
- Bañuelos, R., & Smits, R. G. (1997). Brownian motion in cones. *Probability theory and related fields*, 108(3), 299–319.

- Basel Committee on Banking Supervision. (2005). *An explanatory note on the basel ii irb risk weight functions* (tech. rep.) (ISBN 92-9131-673-3). Bank for International Settlements. Basel, Switzerland. <https://www.bis.org/bcbs/irbriskweight.pdf>
- Basel Committee on Banking Supervision. (2006). *Studies on credit risk concentration: An overview of the issues and a synopsis of the results from the research task force project* (Basel Committee on Banking Supervision Working Paper No. 15). Bank for International Settlements.
- Burtschell, X., Gregory, J., & Laurent, J.-P. (2007). Beyond the gaussian copula: Stochastic and local correlation. *Journal of Credit Risk*.
- Casellina, S., Salis, F., Tessitore, G., Ugoccioni, R., & Varetto, F. (2023). *The calibration of the irb supervisory formula – a case study* (EBA Staff Paper Series No. 17) (EBA Staff Paper Series No. 17 – 09/2023). European Banking Authority.
- Corcóstegui, C., González-Mosquera, L., Marcelo, A., & Trucharte, C. (2003). *Analysis of procyclical effects on capital requirements derived from a rating system* (tech. rep.). Banco de España.
- Da Fonseca, J., Gnoatto, A., & Grasselli, M. (2015). Analytic pricing of volatility-equity options within wishart-based stochastic volatility models. *Operations Research Letters*, 43(6), 601–607.
- Da Fonseca, J., & Grasselli, M. (2011). Riding on the smiles. *Quantitative Finance*, 11(11), 1609–1632.
- Da Fonseca, J., Grasselli, M., & Ielpo, F. (2011). Hedging (co) variance risk with variance swaps. *International Journal of Theoretical and Applied Finance*, 14(06), 899–943.
- Da Fonseca, J., Grasselli, M., & Ielpo, F. (2014). Estimating the wishart affine stochastic correlation model using the empirical characteristic function. *Studies in Nonlinear Dynamics & Econometrics*, 18(3), 253–289.
- Düllmann, K., Scheicher, M., & Schmieder, C. (2007). *Asset correlations and credit portfolio risk: An empirical analysis* (Discussion Paper, Series 2: Banking and Financial Studies No. 13/2007). Deutsche Bundesbank.
- Fonseca, J. D., Grasselli, M., & Tebaldi, C. (2007). Option pricing when correlations are stochastic: An analytical framework. *Review of Derivatives Research*, 10(2), 151–180.
- Gnoatto, A., & Grasselli, M. (2014). The explicit laplace transform for the wishart process. *Journal of Applied Probability*, 51(3), 640–656.
- Goodhart, C., & Segoviano, M. (2004). *Basel and procyclicality: A comparison of the standardised and irb approaches to an improved credit risk method* (Discussion Paper No. 524). Financial Markets Group, London School of Economics.
- Gordy, M. B. (2003). A risk-factor model foundation for ratings-based bank capital rules. *Journal of financial intermediation*, 12(3), 199–232.
- Gordy, M. B., & Lütkebohmert, E. (2013). Granularity adjustment for regulatory capital assessment. *International Journal of Central Banking*, 9(3), 33–71.

- Grasselli, M., & Miglietta, G. (2016). A flexible spot multiple-curve model. *Quantitative Finance*, 16(10), 1465–1477.
- Hull, J. C., Predescu, M., & White, A. (2005). The valuation of correlation-dependent credit derivatives using a structural model. *Available at SSRN 686481*.
- Lee, C.-F., Lin, C.-H., & Yang, H.-Y. (2011). The asymmetric behavior and procyclical impact of asset correlations. *Journal of Banking & Finance*, 35(10), 2559–2568. <https://doi.org/10.1016/j.jbankfin.2011.02.006>
- Lopez, J. A. (2002). *The empirical relationship between average asset correlation, firm probability of default, and asset size* (tech. rep.). Federal Reserve Bank of San Francisco.
- Ma, J. (2009). Pricing foreign equity options with stochastic correlation and volatility. *Annals of Economics & Finance*, 10(2).
- Majumdar, S., & Laha, A. K. (2024). Diffusion on the circle and a stochastic correlation model. *arXiv preprint arXiv:2412.06343*.
- Merton, R. C. (1974). On the pricing of corporate debt: The risk structure of interest rates. *The Journal of finance*, 29(2), 449–470.
- Metzler, A. (2020). State dependent correlations in the vasicek default model. *Dependence Modeling*, 8(1), 298–329.
- Sacerdote, L., Tamborrino, M., & Zucca, C. (2016). First passage times of two-dimensional correlated processes: Analytical results for the wiener process and a numerical method for diffusion processes. *Journal of Computational and Applied Mathematics*, 296, 275–292.
- Tarashev, N., & Zhu, H. (2008). Specification and calibration errors in measures of portfolio credit risk: The case of the asrf model. *International Journal of Central Banking*, 4(2), 129–173.
- Teng, L., Ehrhardt, M., & Günther, M. (2016a). Modelling stochastic correlation. *Journal of Mathematics in Industry*, 6(1), 2.
- Teng, L., Ehrhardt, M., & Günther, M. (2016b). On the heston model with stochastic correlation. *International Journal of Theoretical and Applied Finance*, 19(06), 1650033.
- Vasicek, O. (2002). The distribution of loan portfolio value. *risk*, 15(12), 160–162.